LOWLAND TECHNOLOGY INTERNATIONAL Vol. 11, No. 2, 14-20, December 2009
International Association of Lowland Technology (IALT), ISSN 1344-9656

ELASTO-PLASTIC ANALYSIS FOR DISPLACEMENTS OF GRANULAR PILE ANCHORS (GPA) IN NON-HOMOGENOUS GROUND

B. Vidyaranya,[1] M.R Madhav[2] and M. Kumar[3]

ABSTRACT: Granular piles improve the behavior of the soil by increasing bearing capacity, accelerate consolidation, reduce settlements, and mitigate liquefaction related damages by reinforcement and densification effects. Granular piles can be made to resist pullout or uplift forces by placing an anchor at the base and attaching the same by a cable or rod to the footing to transfer the applied pullout forces to the bottom of the GP termed Granular Pile Anchor (GPA). The elasto-plastic response of GPA in non-homogenous ground is presented considering the shear stress at the interface to be limited to the undrained strength of the soil.

Keywords: Granular piles, elasto-plastic response, compression, pullout, rigid and compressible piles.

INTRODUCTION

Granular piles offer a valuable technique under suitable conditions for increasing the bearing capacity of foundations and stability of embankments founded on soft ground, in reducing settlement and increasing the time-rate of consolidation. The utility of the granular piles is restricted as they can only transfer compressive loads and/or resist shear stresses.

Granular piles can be made to resist pullout or uplift forces by a simple modification of placing an anchor at the base and attaching the same by a cable or rod to the footing to transfer the applied pullout force to the bottom of the GP. Such an assembly is termed a Granular Pile Anchor (GPA). Tests on model granular pile anchors in expansive and soft soils are reported by Kumar (2002 & 2003). Granular pile treated expansive soil adjusts itself to changes in moisture better than an untreated-soil (Phani Kumar *et al.* 2004, Sharma *et al.,* 2004 & 2005, Setty *et al.* 2000 and Hari Krishna *et al.* 2007). The application of reinforced geopiers for resisting tensile loads and settlement control was studied by White *et al.* (2001). Lillis *et al.* (2004) reported results from in situ tests on pullout response of GPA. Kumar *et al.* (2004) and Ranjan *et al.* (2000) present results from laboratory and field tests on pullout response of GPA in cohesive and cohesionless soils. Linear analysis of GPA was reported by Madhav *et al.* (2005 & 2008).

PROBLEM DEFINITION

A granular pile of length, L, and diameter, d, with the soil and pile material characterized by moduli of deformation E_s and E_{gp}, and unit weights of γ_s and γ_{gp}, respectively is considered (Fig.1). The Poisson's ratio of the soil is v_s. A force, Po, applied at the base of GPA is resisted by the shear stress, τ, acting along the periphery of the pile. The force and the stresses acting on and the displacements (upward movements) of the GPA are depicted in Fig. 2a. The shear stresses vary with depth, z. The displacements for a compressible pile increase with depth from a value of ρ_{u0} at the top to ρ_{uL} at the tip.

The stresses transferred to the in situ soil are shown

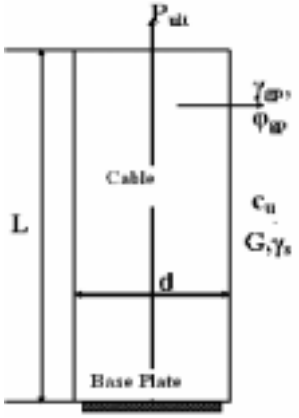

Fig. 1 GPA under Pullout

[1] Osmania University, INDIA
[2] IALT Member, JNTU college of Engineering , Hyderabad, INDIA
[3] Osmania University, INDIA
Note: Discussion on this paper is open until June 2010

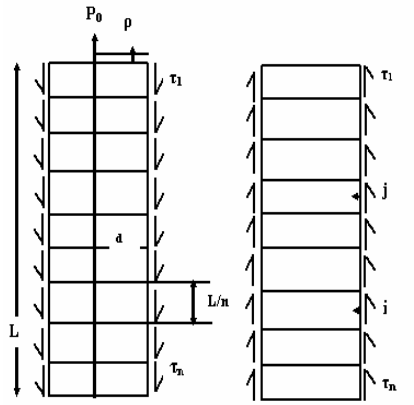

(a) (b)

Fig. 2 Forces and Stresses acting on GPA and Soil**.**

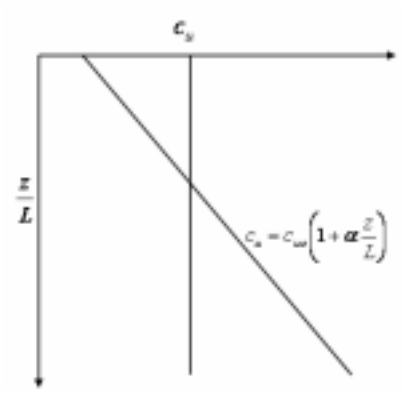

Fig. 3 Variation of undrained shear strength with depth

in Fig. 2b. In order to evaluate the upward displacements of the elements of the soil adjacent to the GPA due to the boundary stresses, τ, function of undrained shear strength of the soil. The undrained shear strength of the soil increases linearly with depth (Fig. 3). The non-homogeneity factor, α, i.e. the rate of increase of undrained strength with depth is taken as 0.25. The GPA surface is divided in to '*n*' elements of length, *L* (=*L/n*). The stress acting on a typical element, *j*, is τj. The displacement at the centre of an element, *i*, due to stresses acting on element, *j*, are obtained by the method described by Poulos and Davis (1980).

Integrating numerically, the Mindlin's equation (1936) for a point load in the interior of a semi-infinite elastic continuum over the periphery of the element, the displacement, $\rho_{s,ij}$, of the soil adjacent to the centre of the i^{th} element due to stress, τ_j, acting on the element, *j*, is

$$\rho_{s,ij} = \frac{d}{E_S} I_{S,ij} . \tau_j \tag{1}$$

where $I_{s,ij}$ – is the soil displacement influence coefficient. The total soil displacement, $\rho_{s,i}$, adjacent to node '*i*' due to stresses on all the elements of the GPA, is obtained by summing up all the displacements at node '*i*', due to stresses on elements *j*=1 to *n*. The soil displacements adjacent to all the nodes are collated to arrive at

$$\{\rho_s\} = \frac{d.[I_s]\{\tau\}}{E_s} \tag{2}$$

where $\{\rho_s\}$ and $\{\tau\}$ are respectively the displacement and shear stress vectors of size, *n*, and $[I_s]$ the displacement influence coefficient matrix of size *n*x*n*.

DISPLACEMENTS OF GPA

The vertical displacements of GPA are obtained considering it to be a compressible pile. Figure 4 depicts the stresses on an infinitesimal element of GPA of thickness, Δz. Poulos and Davis (1980) and Mattes (1969) have established that lateral/radial stresses have negligible effect on the vertical displacements.

The equilibrium of forces in the vertical direction reduces to

$$\frac{d\sigma_z}{dz} - \frac{4}{d}\tau = 0 \tag{3}$$

where σ_z is the normal stress in the GPA. The stress-strain relationship for the GPA material, is

$$\sigma_z = E_{gp} . \varepsilon_z = E_{gp} . \frac{d\rho_{gp}}{dz} \tag{4}$$

where ε_z and ρ_{gp} are respectively the axial strain and GPA displacement. For a homogenous GPA, E_{gp} is constant. Combining Eqs. (3) and (4) and simplifying one gets

$$E_{gp} \frac{d^2\rho_{gp}}{dz^2} - \frac{4}{d}\tau = 0 \tag{5}$$

Equation (5) is solved along with the boundary conditions: *z*=0 (i.e. at the top of GPA) *P*=0 and *z* =*L*(tip of the GPA), *P*=P_0 (the applied load). Since Eq.(5)

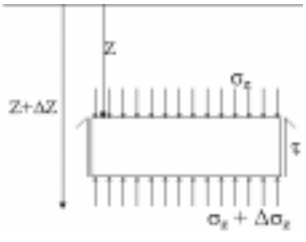

Fig. 4 Stresses acting on an Infinitesimal Element

cannot be integrated directly, its finite difference form is

$$\frac{\rho_{gp,i-1} - 2\rho_{gp,i} + \rho_{gp,i+1}}{(\Delta L)^2} - \frac{4}{E_{gp}.d}\tau_i = 0 \qquad (6)$$

where $\rho_{gp,i}$ and τ_i are respectively the displacement at the centre of node 'i' and the shear stress on the interface of element, 'i', of the GPA.

Equation (6) can be written for nodes i = 2 to (n-1). Invoking the first boundary condition, P = 0 implies σ_z = 0 and hence ε_z = 0 leads to

$$\rho_{gp,1'} = \rho_{gp,1} \qquad (7)$$

where $\rho_{gp,1'}$ – is the displacement at the imaginary node 1' above the GPA. Equation (6) can now be written for node 1 as well. All the equations for nodes 1 to (n-1) are collated and written as

$$[I_{gp}]\{\rho_{gp}\} - \frac{4.L^2}{E_{gp}.n^2.d}.\{\tau\} = 0 \qquad (8)$$

$$\begin{bmatrix} -1 & 1 & 0 & . & . & . & . & . & . & 0 \\ 1 & -2 & 1 & 0 & . & . & . & . & . & 0 \\ 0 & 1 & -2 & 1 & 0 & .. & . & . & . & 0 \\ 0 & 0 & 1 & -2 & 1 & 0 & . & . & . & 0 \\ . & . & . & . & . & . & . & . & . & . \\ . & . & . & . & . & . & . & . & . & . \\ . & . & . & . & . & . & . & . & . & .. \\ . & . & . & . & . & . & . & . & . & . \\ . & . & . & . & . & . & 1 & -2 & 1 & \end{bmatrix} \qquad (9)$$

where $[I_{gp}]$ is the GPA displacement influence coefficient matrix, of size nx(n-1),

COMPRESSIBLE PILE

The soil and pile displacement equations are normalized with diameter, d, and undrained shear strength c_{u0} to get dimensionless quantities as

Soil displacement equation	Pile displacement equation
$\{\rho_s^*\} = \frac{c_{uo}}{E_s}[I_s]\{\tau^*\}$	$[I_p]\{\rho_p^*\} - \frac{4.(L/d)^2.c_{uo}}{E_{gp}.n^2}[1]\{\tau^*\} = 0$ (10)

where $\left\{\rho_s/d\right\} = \rho^*$ $\qquad$ $\left\{\tau/c_{uo}\right\} = \tau^*$

But the compatibility of displacements requires

$$\{\rho_p^*\} = \{\rho_s^*\} \qquad (11)$$

The pile displacement equation is written as

$$[I_p]\{\rho_s^*\} - \frac{4.(L/d)^2}{(E_{gp}/c_{u0}).n^2}[1]\{\tau^*\} = 0 \qquad (12)$$

which reduces to

$$[I_p]\{\rho_s^*\} - \mu[1]\{\tau^*\} = 0 \qquad (13)$$

where $\mu = \frac{4.(L/d)^2}{(E_{gp}/E_s)(E_s/c_{u0}).n^2}$

Load, P_0, at $z = L$, is expressed as

$$E_{gp}.\frac{\rho_{n+1} - \rho_n}{\Delta z}.\frac{\pi.d^2}{4} = P_0 \qquad (14)$$

where ρ_{n+1} is the displacement at the imaginary node below node 'n'. The ultimate pullout load, $P_{ult} = \pi.d.L.c_{u0}(1+\alpha/2)$. Normalizing P_0 with $\pi.d.L.c_{uo}$ and the displacements with diameter, d, Eq. (14) becomes

$$\{\rho_{n+1}^* - \rho_n^*\} = \frac{4.P_0^*.(L/d)^2}{(E_{gp}/c_{uo}).n} \qquad (15)$$

where Eq. (15) can be written as

$$\{\rho_{n+1}^* - \rho_n^*\} = n.\mu.P_0^* \qquad (16)$$

Where $\mu = \frac{4.(L/d)^2}{(E_{gp}/E_s)(E_s/c_{u0}).n^2}$

Equations 10, 12 & 16 are combined to solve for the shear stresses and the displacements, as

$$\begin{bmatrix} [1] & \frac{-1}{(E_s/c_u)}[I_s] \\ [I_p] & -\mu.[1] \end{bmatrix} \begin{Bmatrix} \rho_s^* \\ \tau^* \end{Bmatrix} = \begin{Bmatrix} 0 \\ 0 \\ 0 \\ n.\mu.P^* \end{Bmatrix} \qquad (17)$$

RIGID PILES

For rigid piles Eq. (17) reduces to Madhav and Poorooshasb (1989) as

$$\begin{bmatrix} [I_s]\left\{\tau/c_u\right\} & -\left(E_s/c_u\right)[1]\delta^* \\ [1]\left\{\tau/c_u\right\} & -0.\delta_0 \end{bmatrix} \begin{Bmatrix} \tau^* \\ \delta^* \end{Bmatrix} = \begin{Bmatrix} 0 \\ 0 \\ 0 \\ n.P^* \end{Bmatrix} \qquad (18)$$

Elasto-Plastic Response

The shear stress, τ_i, on any element, 'i', cannot exceed the undrained strength, $c_{uo}(1+\alpha(z/L))$, i.e.

$$\tau_i \le c_{uo}\{1+\alpha.(z_i/L)\} \qquad (19)$$

and the i^{th} row in Eq. (19) is replaced with

$$\{0\ \ 0\ \ .\ \ .\ \ 1\ \ 0\ \ 0\}\{\tau_i^*\}=1+\alpha(z_i/L)) \qquad (20)$$

and the set of equations solved. Yielding generally starts from the tip, and progresses towards the top. In some particular cases, yielding of the top element gets initiated after some elements in the lower part of GPA have yielded after some stage of loading.

RESULTS

The elasto-plastic behavior of GPA is studied by solving Eqs. (17) & (18) for the following ranges of parameters for both rigid and compressible piles for homogenous and non-homogenous conditions: L/d = 5, 10, 20, 25, 50; E_s/c_{u0} = 100, 200, 300, 500 & 1000; E_{gp}/E_s = 10, 20, 50, 100, 200, 500, 2000, 5000; v_s=0.5; non-homogeneity co-efficient, α=0 and 0.25.

VARIATION OF SHEAR STRESSES

The pullout load, P_0, is applied in increments until shear stress along each elemental surface along the total pile length reaches the undrained shear strength corresponding to that depth. The variations of shear stresses with depth, z, at different P^* values for a rigid pile with L/d=10, and E_s/c_{u0} = 200 are shown in Fig. 5. The shear stresses are nearly constant with depth at small values of P^* (< 0.3) and increase sharply near the tip as noted by Madhav and Poorooshasb (1989) for piles under tension and Poulos and Davis (1968) for piles under compression both behaving linearly. Yielding begins near the tip with increasing P^* values and proceeds towards the top. At P^*= 0.4, the yielding starts at depth close to diameter'd' from the toe and increases steeply. The variation is nearly constant for homogenous and non-homogenous condition at smaller values of P^*. At P^*=0.98, the stress in the homogenous condition yield near the top of GPA and near constant with increasing depth. For the same pullout load the variation of the shear stress with depth increase steadily and increase steeply beyond z/L=0.7 as the stresses start yielding.

Variations of shear stresses with depth (Fig. 6) for a compressible GPA with E_{gp}/E_s=100 and for the same parameters as for the rigid pile are very similar once again to those for the rigid pile. The differences in the normalized shear stress variations for homogenous and non-homogenous conditions increase with increasing values of P^*. At smaller values of P^*= 0.685 the stresses increases steadily up to 0.75 and then increase steeply to the maximum yield stress. The yielding of the stress proceed towards the top with increasing pullout load. At P^*=0.999, the stresses starts yielding from a depth close to z/L= 0.45. The behavior of the variation of the stresses is similar in rigid pile and GPA with increasing pullout load but the variations are more with increasing depth for the GPA.

The variations of the shear stress with normalized depth for P^*=0.69 for compressible pile for different values of L/d and for E_{gp}/E_s = 100, E_s/c_{u0}=200 and v_s =0.5 are presented in Fig. 7**.** Shear stresses at more number of elements or over longer lengths of the GPA yield for longer GPA than those for shorter ones. For L/d =50 the yielding starts at a depth z/L=0.45 and increase with depth. Shear stresses over more than fifty percent of the pile length have yielded for L/d of 50 at P*=0.69 while only thirty percent of the pile length has yielded

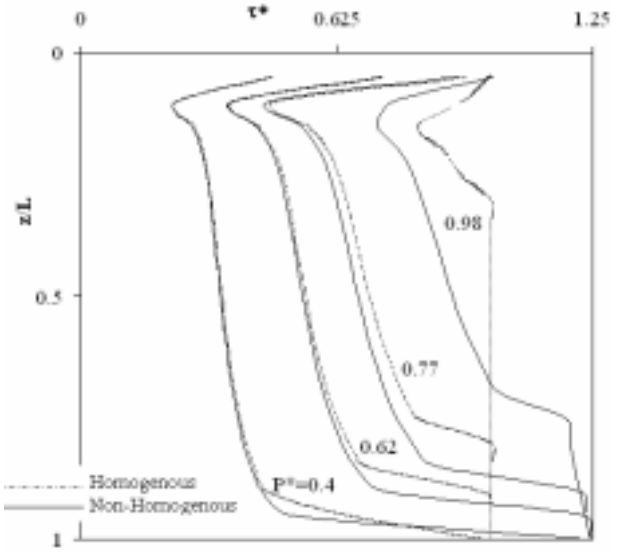

Fig. 5 Variation of τ* vs. z/L for L/d = 10 for E_s/c_u=200 and v_s= 0.5 with increasing P^*-Rigid Pile

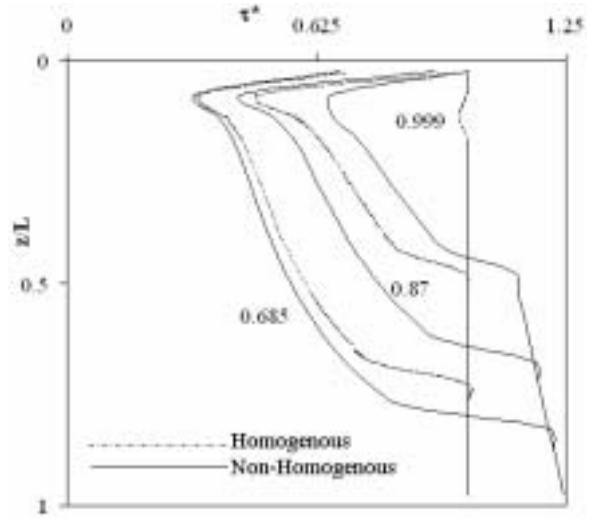

Fig. 6 Variation of τ* vs. depth for L/d = 10, E_s/c_u = 200, E_{gp}/E_s = 100 for ν_s = 0.5 for GPA

elements for *L/d* of 5. Hence the shear stresses mobilized along the non-yielded elements are more for short GPA (*L/d*=5) and decrease at these depths with increasing values of *L/d*.

The influence of the relative stiffness factor, *K* (=E_{gp}/E_s), on the shear stress variations with depth for P^* of 0.69 is presented in Fig. 8 for *L/d*=10, E_s/c_{u0}=100, and ν_s=0.5.

The differences in the shear stresses for homogenous and non-homogenous conditions decrease with increasing *K*. At *K*=10, more stresses have yielded at depth, *z/L*= 0.4 and increase with increasing depth. For increasing *K* values the yielding of the stresses decrease with depth. For *K*= 50 the yielding starts at a depth of 0.65 and for *K*= 5000 it is at 0.85.

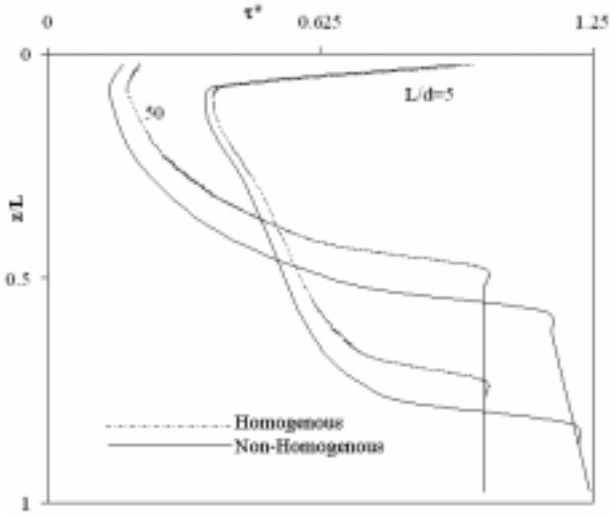

Fig. 7 Variation of τ^* vs. Depth for P^* = 0.69, E_{gp}/E_s = 100, E_s/c_u =200 and ν_s = 0.5-effect of *L/d* for GPA

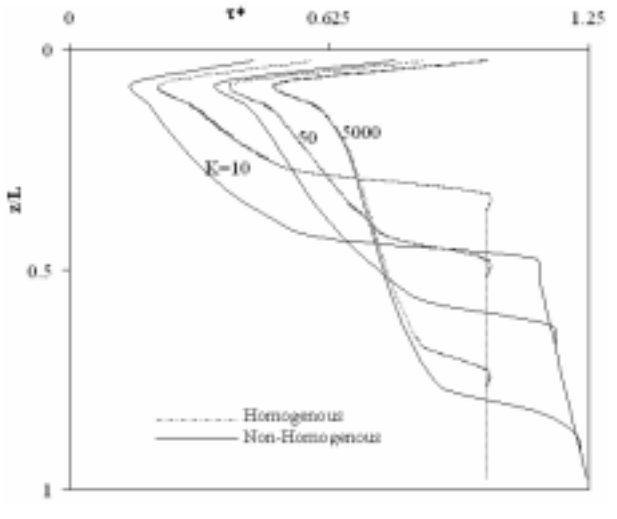

Fig. 8 Variation of τ^* with depth for E_s/c_u = 100 and ν_s= 0.5and *L/d*=10 - Effect of *K*(=E_{gp}/E_s) for GPA

LOAD - DISPLACEMENT RESPONSES

The displacements generated along the pile length are extrapolated to obtain the top and tip displacements considering the 1st, 2nd & 3rd elements for the top and *n*-2, *n*-1& *n*th elements displacement in GPA, respectively. The variations of the normalized load, *P** (normalized with $\pi d^2 c_{u0}/4$ to eliminate the effect of *L/d* in the normalization of pullout load) with normalized tip displacement, δ^*= (ρ/d) for rigid and compressible piles are shown in Figs. 9 & 10 respectively for E_s/c_{u0} =200 and ν_s=0.5 for different ratios of *L/d*.

The normalized displacements for a given *P** increase with increasing values of *L/d*. The displacements generated in *L/d* = 5 at P^*=30 are of the order 0.022. And the displacements generated in GPA increase with increasing *L/d*. For *L/d*=20, at P^*= 80, the

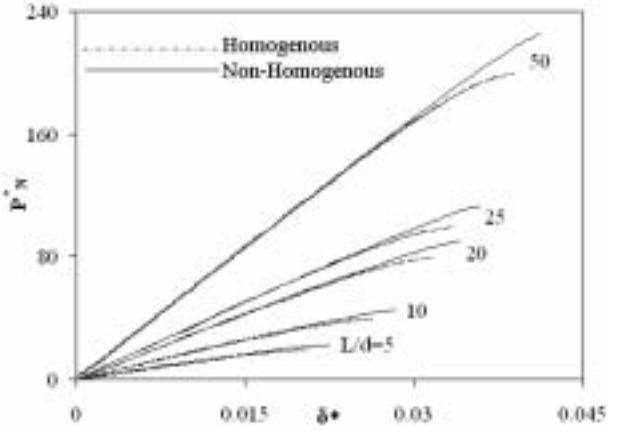

Fig. 9 Variation of P^*_N with δ^* for E_s/c_u= 200 and ν_s=0.5 - Effect of *L/d* - rigid piles

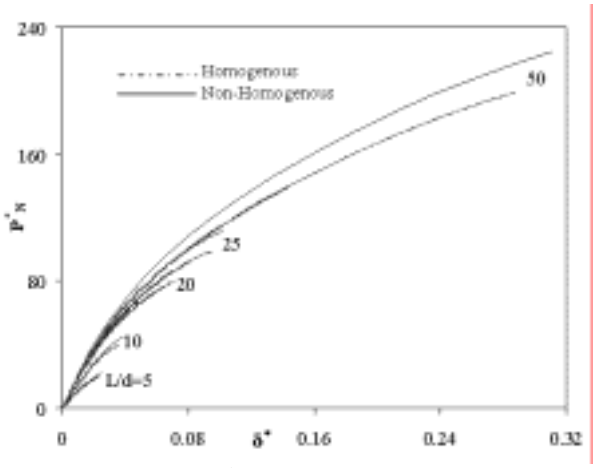

Fig. 10 Variation of P^*_N with δ* for E_{gp}/E_s =100, ν_s= 0.5, and E_s/c_u=200, – for Effect of L/d –GPA

normalized displacements generated are close to 0.035. And for L/d =50, the P^* increases to 210 and also the displacements are 0.04.

Pullout load increases by about five folds and displacements by two folds with increase in L/d from 5 to 50. Longer piles exhibit larger tip displacements compared to shorter ones at a given normalized pullout force.

The normalized pullout force – tip displacement plots for GPA (Fig. 10) are very similar to those for rigid piles (Fig.9) except that the displacements are very large for GPA since the relative stiffness factor, K= 100.

The displacements for L/d =5 are very negligible and are of the order 0.02 for P^* = 20 and the displacements increase with increasing L/d. For L/d =50 the displacements generated are close to 0.26 at a pullout load, P^*=200.

The influence of the E_s/c_{u0} on the variation of tip displacement, δ^* with P^* is presented in Figs. 11 & 12 for L/d = 10 for rigid piles and compressible GPA. The displacements generated at E_s/c_{u0}=100 are of the order 0.058 and decrease with increasing E_s/c_{u0} and are close to 0.005 for E_s/c_{u0} = 5000.

The displacements generated for higher values of E_s/c_{u0} are constant with increasing pullout load, P^*. Displacements are very sensitive to E_s/c_{u0} reducing by several orders of magnitude for E_s/c_{u0} increasing from 100 to 5,000.

The effect of K (= E_{gp}/E_s) for L/d=10 on pullout load versus tip displacement plots is studied in Fig. 13. With increasing E_s/c_{u0} the displacements reduce and the GPA behaves like an incompressible pile.

The effect is similar to the rigid pile but the magnitudes of the displacements generated are higher to the rigid piles. For K (E_s/c_{u0}) =100 the displacements generated are close to 0.11 for P^* = 1.0 and decrease to 0.01 for P^*=1.15.

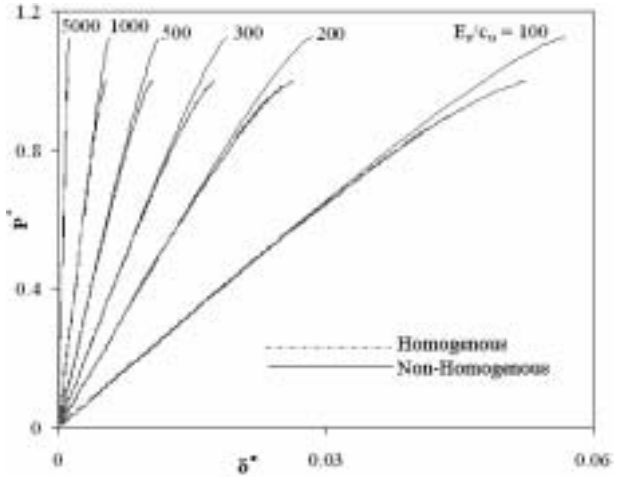

Fig. 11 Variation of P^* with δ^* for L/d = 10 & ν_s = 0.5 – Effect of E_s/c_u – Rigid Piles

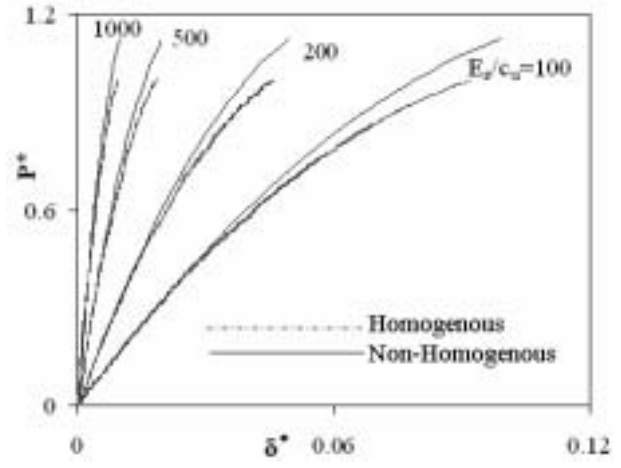

Fig. 12 Variation of P^* with δ^* for L/d = 10, E_{gp}/E_s= 50 & ν_s= 0.5 –Effect of E_s/c_u-GPA

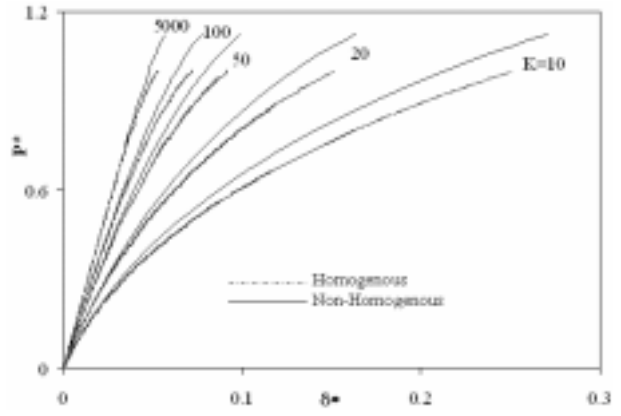

Fig. 13 Variation of P^* with δ^* for L/d = 10, E_s/c_u=100-Effect of K (=E_{gp}/E_s)

CONCLUSIONS

An analysis of GPA is presented considering the GPA - in situ soil interface response to be elasto-plastic,

i.e. the interface shear stresses are limited to the undrained strength of the soil which increases linearly with depth. The elastic continuum approach of Poulos and Davis (1980) is extended to predict the pullout load – displacement responses of GPA. A parametric study has been carried out and the results in the form of variations of normalized shear stress, displacements and of normalized axial uplift force with depth with relative stiffness factor, K ($=E_{gp}/E_s$) and E_s/c_{u0} are presented for rigid and compressible piles. The salient conclusions are:

1. Granular Pile Anchors (GPA) are very effective in transferring applied loads to strata at depth particularly if they are relatively long and/or more compressible.
2. For relative stiffness factor K>1,000, a compressible GPA behaves like an incompressible or a rigid pile.
3. The effect of non-homogeneity of strength profile on the response of GPA is significant. While the normalized load-displacement curves are close to each other for homogeneous and non-homogeneous cases, it should be remembered that the ultimate capacities with which the load is normalized are different for the two cases.
4. GPA transfers larger shear stresses near the toe where the in situ strength is maximum in case of non-homogeneous ground.
5. The effect of non-homogeneity on normalized load – displacement response is particularly significant in case of more compressible GPA (K=10).

REFERENCES

Hari Krishna P. and Ramana Murthy V. (2007). In situ Heave Control of Model Walls Using Granular Anchor Piles. 13th ARC, Kolkota, India. Part-I, Paper No. 42.

Kumar, P. (2002). Granular Anchor Pile System under Axial Pullout Loads. Ph.D. Thesis, I.I.T. Roorkee.

Kumar, P., Ranjan, G. and Saran, S. (2003). GAP System for Resistance of Uplift Forces – A Field Study. Proc. Indian Geotechnical Conference, Roorkee: 597-602.

Kumar, P., Ranjan, G. and Saran, S. (2004). Granular Pile System for Strengthening of Weak Sub-Soils –A Field Study. Proc. of ICGGE; IIT Bombay: 217-222.

Lillis, C., Lutenegger, A.J and Adams, M. (2004). Compression and Uplift of Rammed Aggregate Piers in Clay. Geosupport: 497-507.

Mindlin, R.D. (1936). Force at a point in the Interior of a Semi-infinite Solid. Physics 7: 195.

Madhav, M.R., and Poorooshasb, H.B. (1989). Pile Displacement Due to Tensile Loads. Indian Geotechnical Journal, Vol.18 (1): 48-53.

Madhav, M.R., Vidyaranya, B. and Sivakumar, V. (2005). Ultimate Pullout Resistance and Displacements under Working Loads of GPA, Keynote Lecture, Indian Geotechnical Conference, Ahmedabad: 45-52.

Madhav, M.R., Vidyaranya, B. and Sivakumar, V. (2008). Linear Analysis and Comparison of Displacements Granular Pile Anchors. Ground Improvement Journal, Issue 161: 31- 41.

Mattes, N.S. (1969). The Influence of Radial Displacement Compatibility on Pile Settlement. Geotechnique.Vol.19: 157-159.

Phani Kumar, B.R., Sharma, R.S., Srirama Rao, A. and Madhav, M.R. (2004). Granular Pile Anchor Foundation (GPAF) System for Improving the Engineering Behaviour of Expansive Clay Beds. Geotechnical Testing Journal, ASTM, Vol.27, No.3: 1-9.

Poulos H.G., and Davis, E.H. (1968). "The settlement behavior of single axially loaded incompressible piles and piers".Geotechnique, 18,351-371.

Poulos, H.G. and Davis, E.H. (1980). Pile Foundation Analysis and Design. John Wiley and Sons, New York: 397.

Ranjan, G. and Kumar, P. (2000). Behaviour of Granular Piles under Compressive and Tensile Loads. Geotechnical Engineering, J. of SEAGS, Vol.31, No.3: 209.

Setty Narayanaswamy, K.R., Ravi Shanker, A.U. and Narasimha Reddy, G.N. (2000). Uplift Behaviour of Granular Pile-Anchors in Expansive Soils. Indian Geotechnical Conference, Bombay: 305-306.

Sharma, R.S., Phanikumar, B.R. and Nagendra. (2004). Compressive Load Response of Geogrid Reinforced Granular Piles in Soft Clays. Canadian Geotechnical Journal, Vol.41: 187-192.

Sharma, R.S. and Phanikumar, B.R. (2005). Laboratory Study of Heave Behaviour of Expansive Clay Reinforced with Geopiles. Journal of Geotechnical & Geo-environmental Engineering, ASCE, Vol. 131, No.4:512-520.

White, D., Wissmann, K., and Lawton, E. (2001). Geopier Reinforcement for Transportation Application. Geotechnical News: 63-68.